

# An experimental investigation on spray, ignition and combustion characteristics of biodiesels

Xiangang Wang, Zuohua Huang \*,

State Key Laboratory of Multiphase Flow in Power Engineering, Xi'an Jiaotong University, Xi'an 710049, China

Olawole Abiola Kuti, Wu Zhang, Keiya Nishida

Department of Mechanical System Engineering, University of Hiroshima, 1-4-1 Kagamiyama, Higashi-Hiroshima 739-8527, Japan

## Corresponding author:

Zuohua Huang

State Key Laboratory of Multiphase Flow in Power Engineering

Xi'an Jiaotong University, Xi'an 710049, China

Tel: +86-29-82665075, Fax: +86-29-82668789

E-mail: [zhhuang@mail.xjtu.edu.cn](mailto:zhhuang@mail.xjtu.edu.cn)

**Colloquium topic:** Spray and droplet combustion

## Paper length (method 1):

<b>Main Text:</b>	word processor count	<b>3119</b>
<b>References:</b>	(29+2) x (2.3 lines/reference)x(7.6 words/line)	542
<b>Figure Captions:</b>	word processor count	109
<b>Table 1:</b>	(10 lines + 2 lines) x (7.6 words/line) x (1columns)	<b>92</b>
<b>Fig. 1:</b>	(77 mm+10)x(2.2 words/mm)x(2 column)	383
<b>Fig. 2:</b>	(60 mm+10)x(2.2 words/mm)x(1 column)	154
<b>Fig. 3:</b>	(50 mm+10)x(2.2 words/mm)x(1 column)	132
<b>Fig. 4:</b>	(67 mm+10)x(2.2 words/mm)x(1 column)	169
<b>Fig. 5:</b>	(50mm+10)x(2.2 words/mm)x(1 column)	132
<b>Fig. 6:</b>	(50 mm+10)x(2.2 words/mm)x(1 column)	132
<b>Fig. 7:</b>	(48 mm+10)x(2.2 words/mm)x(1 column)	128
<b>Fig. 8:</b>	(50 mm+10)x(2.2 words/mm)x(1 column)	132
<b>Fig. 9:</b>	(50 mm+10)x(2.2 words/mm)x(1 column)	132
<b>Fig. 10:</b>	(58 mm+10)x(2.2 words/mm)x(1 column)	150
<b>Fig. 11:</b>	(50 mm+10)x(2.2 words/mm)x(1 column)	132
	<b>Total</b>	<b>5637</b>

# **An experimental investigation on spray, ignition and combustion characteristics of biodiesels**

**Xiangang Wang, Zuohua Huang \***,

State Key Laboratory of Multiphase Flow in Power Engineering, Xi'an Jiaotong University, Xi'an 710049, China

**Olawole Abiola Kuti, Wu Zhang, Keiya Nishida**

Department of Mechanical System Engineering, University of Hiroshima, 1-4-1 Kagamiyama, Higashi-Hiroshima 739-8527, Japan

**Abstract:** Spray, ignition and combustion characteristics of biosiesel fuels were investigated under a simulated diesel-engine condition (885K, 4MPa) in a constant volume combustion vessel. Two biodiesel fuels originated from palm oil and used cooking oil were used while JIS#2 used as the base fuel. Spray images were taken by a high speed video camera by using Mie scattering method to measure liquid phase penetration and liquid length. An image intensifier combined with OH filter was used to obtain OH radical image near 313 nm. Ignition and combustion characteristics were studied by OH radical images. Biodiesel fuels give appreciably longer liquid lengths and shorter ignition delays. At low injection pressure (100 MPa), biodiesel fuels give shorter lift-off lengths than those of diesel. While at high injection pressure (200 MPa), the lift-off length of biodiesel fuel originated palm oil gives the shortest value and that of biodiesel from used cooking oil gives the longest one. Air entrainment upstream of lift-off length of three fuels was estimated and compared to soot formation distance. This study reveals that the viscosity and ignition quality of biodiesel fuel have great influences on jet flame structure and soot formation tendency.

**Keywords:** Biodiesel; Spray; Ignition; Combustion; Lift-off length.

## 1. Introduction

Flame combustion process in DI diesel engine has been investigated extensively using the optical diagnostics. A number of fundamental investigations on diesel jet flame were conducted by Dec, Siebers and Pickett et al. at Sandia National Laboratories [1-14]. Dec [3] proposed a conceptual model of diesel spray combustion after conducting a number of researches in a heavy-duty optical diesel engine. The conceptual model describes the details of fuel mixing, vaporization, combustion and soot formation. Siebers et al. [4-14] added detailed quantitative empirical models for the reacting jets by studying fuel jet ignition, penetration, and lift-off length in a constant volume combustion vessel.

As fuel is injected into the combustion chamber of diesel engine, hot ambient air will be entrained from the surrounding ambient gases, forming a liquid phase core-shaped spray. Siebers et al. [6] found that modern injection pressures were high enough for spray atomization, and fuel evaporation was not limited by spray atomization but rather by the rate of hot air entrainment. During the quasi-steady period, the tip of spray liquid phase stays a mean axial location, which is defined as liquid length. Siebers et al. [7-9] studied the effects of injection pressure, ambient temperature and density, nozzle diameter and fuel type on liquid length and proposed a scaling law for liquid length. Moreover, Siebers et al. [10-12] measured flame lift-off of diesel sprays and investigated the effects of ambient conditions, injection pressure, nozzle diameter and fuel type on the lift-off length. Lift-off length was defined as the distance from injector tip to the upstream region of combustion. Siebers and Higgins [10] proposed a schematic diagram to illustrate the effect of engine operation parameters and nozzle diameter on the liquid length, lift-off length and soot formation position and analyzed the relationships among liquid length, lift-off length and soot formation. They concluded that the lift-off length would control the fuel-air premixing prior to

combustion within the rich premixed zone. Pickett and Siebers [13] conducted a comprehensive study on soot formation in diesel fuel jets near the lift-off length. They found that fuel type and air entrainment prior to the lift-off length would significantly affect combustion and soot formation tendency. Pickett et al. [14] revealed a strong correlation between the fuel ignition quality and lift-off length.

Biodiesel fuel, as one of alternative diesel fuels, is currently of great interest and an important research subject for soot reduction in diesel engines. Biodiesel fuels contain oxygen and thus provide an effective way to enhance combustion process and inhibit soot formation in diesel engines [15]. This motivates a number of experimental works on combustion and emission characteristics of biodiesel fuel in diesel engines [15-21]. Moreover, biodiesel has different physical and chemical fuel properties compared to those of diesel. These fuel properties may have a complicated impact on spray atomization, evaporation, combustion and soot formation characteristics. Although many studies have been conducted on the effects of biodiesel fuel properties on combustion and emissions, they mainly focused on engine performance rather than on spray and flame characteristics. Few reports on the relationship among liquid length, ignition quality, lift-off length and soot formation characteristics of biodiesel spray were presented. The relationship is beneficial to the interpretation and understanding on soot reduction by biodiesel fuels in diesel engines.

The objective of this study is to examine the spray, ignition and combustion characteristics of biodiesel fuels and to establish the interdependency among liquid length, ignition quality, lift-off length and soot formation of biodiesel sprays. In this work, spray, ignition and combustion processes were studied under a simulated diesel-engine condition (885K, 4MPa) in a constant volume combustion vessel. Two biodiesel fuels originated from palm oil (BDFp) and used cooking oil (BDFc) were used and JIS#2 diesel was used as base fuel. Two injection pressures of 100 and 200

MPa were used. Spray characteristics were studied by Mie-scattering method, and ignition and combustion information were obtained from OH radical flame images. Soot formation information was obtained by two-color pyrometry.

## **2. Experimental apparatus and procedure**

The spray and combustion experiments were conducted under a simulated diesel-engine condition (885 K, 4MPa) in a constant volume combustion vessel. The schematic experimental apparatus is given in Fig.1. This combustion vessel is able to simulate the typical thermodynamic condition in combustion chamber of diesel engine. The high temperature is produced by an electrically heater located in the bottom of combustion chamber. The fuel injection system mainly consists of fuel reservoir, high pressure generator, common rail, injector and control system. A Kistler pressure transducer is fixed inside the common rail to measure injection pressure. The fuel injector is controlled and driven by ECU. The injection time and pulse width is set by delay pulse generator DG535. The injector tip is a single-hole type one with the nozzle diameter of 0.16 mm. It opens and closes rapidly ( $<0.1$  ms) and thus has top-hat injection rate profiles [22].

Mie scattering method was employed to visualize the liquid phase image. A Xenon lamp was used as light source. Two mirrors with adjustable position were used to reflect and focus light on the spray. For combustion study, the Xenon lamp and mirrors were not used any more. An image intensifier coupled with a bandpass filter of a central wavelength at 313 nm (10 nm FWHM) was mounted to the high speed video camera to take the OH radical images of flame.

The ambient temperature and pressure were set to 885 K and 4.0 MPa to simulate the typical thermodynamic condition ( $-10^\circ$  ATDC ) in diesel engine cylinder. For spray study, nitrogen was filling in the combustion vessel as ambient gas. While for combustion study, compressed air was used. Two injection pressures (100 and 200 MPa) were adopted.

Two biodiesel fuels originated from palm oil (BDFp) and used cooking oil (BDFc) were used while JIS#2 was used as base fuel. Table 1 gives the main properties and compositions of biodiesel and diesel fuels.

### 3. Results and Discussion

#### 3.1 Spray characteristics

Fig. 2 shows the samples of spray development processes for BDFp at injection pressures of 100 and 200 MPa. As Mie scattering is used, only liquid phase can be presented. After the start of injection, liquid phase spray penetrates monotonously during an initial development period. However, the liquid phase spray does not develop further beyond a certain distance. The tip of the liquid fuel stops penetrating and fluctuates about a mean axial location. This fluctuation is attributed to spray turbulence. This phenomenon was also observed under high temperature and pressure conditions in the previous works [6-9]. The length of this quasi-steady liquid region is defined as liquid length. In addition, it can be observed that the liquid tip is surrounded by spray mist. This spray mist consists of a number of small liquid droplets and fuel vapor. This phenomenon suggests that the atomization and evaporation processes gradually evolve and there is no distinct boundary between liquid and vapor phase. The liquid phase was defined as the region with intensity above a threshold. The threshold was specially chosen to obtain insensitive trend of liquid phase penetration versus threshold. The liquid length was obtained by averaging the liquid phase penetrations during quasi-steady period.

The liquid length of each condition is given in Fig. 3. The liquid length is insensitive to injection pressure, which is consistent with the mixing limited theory [9]. It is generally recognized that high viscosity and *surface tension* of biodiesel fuels will lead to poor spray atomization [23]. Biodiesel fuels generally have poor fuel volatilities compared to that of diesel fuel [8, 24]. Previous studies

have demonstrated a linear correlation between liquid length and fuel volatility [6, 25]. However, the difference of liquid length among the three fuels is small and ignorable, which needs to be studied further.

### 3.2 Ignition and combustion characteristics

In this study, line-of-sight OH radical images of the flame were used to study the ignition and combustion processes. OH chemiluminescence provides an excellent marker of combustion activity and lift-off length [10-13]. In this study, the start of ignition is defined as the initial appearance of OH radical image. The ignition delay is defined as the duration from the start of injection to the initial emergence of OH radical flame kernel.

Fig. 4 shows the samples of ignition position and flame kernel development for BDFp. The white bar in each image indicates the measured liquid length. Ignition occurs a short distance downstream of the spray liquid tip. In other words, ignition takes place within the vapor phase (or the mixtures of small liquid droplet and vapor). This observation agrees with the current understanding spray combustion process in diesel engines [4-5]. And this is consistent to the results in other studies [26-27]. Moreover, the ignition position of 200 MPa moves downstream compared to that of 100 MPa. This is due to the increased jet velocity with the increase of injection pressure.

Fig. 5 gives the ignition delay of three fuels. The result shows that diesel fuel gives longer ignition delay than those of BDFp and BDFc, while the difference of ignition delay between BDFc and diesel is small and can be ignored, although BDFp and BDFc give higher and lower Cetane numbers than that of diesel respectively. This suggests that only Cetane number cannot provide a reasonable indication of ignition delay in all cases. With the increase of injection pressure, ignition delays of three fuels are shortened. The enhanced fuel-air mixing rates are responsible for the decreased ignition delay.

Ignition occurs at the premixed mixtures of fuel vapor and air. After initial appearance of flame kernel, the flame develops both downstream and upstream, and the projected flame area increases rapidly. Fig.6 shows the variations of OH luminosity area versus elapsed time after the start of ignition. The flame area increases rapidly after ignition occurs and then increases gradually. The rapidly increased flame area reflects rapid burning of fuel-air mixtures. This rapid burning rate at initial stage corresponds to the rapid increased heat-release rate of the premixed combustion in the traditional combustion model of diesel engines.

OH intensity profile along the injector axial line is given in Fig. 7. The threshold value of 10 was selected, and the pixels with intensity lower than 10 were excluded from the analysis. OH intensity profile along injector axial line presents two peaks. The first intensity peak suggests that strong heat-release reaction occurs at upstream combustion location. This strong heat-release reaction is from the fuel-rich partially premixed combustion. Pickett and Siebers also found this phenomenon via line-of-sight OH radical image [13].

### **3.3 Flame lift-off length**

After the initial development of flame kernel, the fuel jet flame turns into a lifted, turbulent diffusion flame during quasi-steady stage, as shown in Fig. 8. The lift-off length is defined as the distance from the injector tip to the most upstream location of combustion in the fuel jet [10]. Flame lift-off allows fuel and air to premix upstream of the lift-off length, which affects the combustion and soot formation processes downstream [12, 13].

The averaged lift-off length, which is obtained during quasi-steady flame duration, is given in Fig. 9. The liquid length is also shown in Fig. 9 for the comparison. Biodiesel fuels give shorter lift-off lengths than that of diesel at injection pressure of 100 MPa. While at injection pressure of 200 MPa, the lift-off length of BDFp is the shortest and that of BDFc is the longest.



Pickett et al. [14] found that the ignition quality of a fuel would affect the lift-off length and fuels with short ignition delay generally produce short lift-off lengths in most cases. High Cetane number and short ignition delay of BDFp indicates easy auto-ignition of BDFp. Thus, the jet flame of BDFp moves more closely to the injector tip. The difference of lift-off length between BDFc and diesel is quite small at injection pressure of 200 MPa. Moreover, the lift-off length increases with the increased injection pressure.

The comparisons of liquid length and lift-off length in Fig. 9 can provide an insight on relationship between fuel vaporization and combustion of fuel spray. At injection pressure of 100 MPa, liquid length is longer than lift-off length for the three fuels. However, at injection pressure of 200 MPa, only BDFp presents a shorter lift-off length than liquid length. The short lift-off length suggests a direct interaction between fuel liquid phase and combustion regions. The liquid phase tip is surrounded by diffusion combustion sheath. Thus, a cold core might exist inside the flame sheath. This cold core is blocked to entrain ambient air by the flame sheath. The lift-off length is longer than liquid length for BDFc and diesel at injection pressure of 200 MPa. This suggests that fuel vaporization is completely finished prior to combustion and no direct interaction between fuel liquid phase and combustion exists. Liquid length is insensitive to injection pressure, but lift-off length is increased with increasing injection pressure especially for BDFc and diesel. This leads to the difference of relative spatial relationship between fuel vaporization and combustion regions.

### **3.4 Estimated air entrainment upstream of lift-off length**

The air entrainment upstream of lift-off length will influence the amount of fuel-air premixing that occurs prior to the initial combustion zone [10]. This fuel-air premixing will affect the composition of reactants in the fuel-rich partially premixed reaction zone in the jet central region, and the soot formation processes downstream of this rich central reaction zone [13]. In this section, a

simple model is used to estimate the air entrainment upstream of lift-off length [28]. The cross-sectional average equivalence ratio at the position of lift-off length can be obtained. The oxygen ratio, introduced by Mueller et al. [29] to account for the difference in mixture stoichiometry of oxygenated fuels, was also acquired. The oxygen ratio is defined as the amount of oxygen available in the fuel-air mixtures divided by the amount needed for stoichiometric combustion.

The cross-sectional average equivalence ratio and oxygen ratio at the position of lift-off length are plotted in Fig. 10. At both injection pressures, BDFp give higher equivalence ratios than those of BDFc and diesel at the lift-off position. The short lift-off lengths in Fig. 9 correspond to large equivalence ratios. Meanwhile, the spray angles of BDFp are smaller than those of BDFc and diesel due to higher viscosity and surface tension [28]. This also leads to less air entrainment upstream of lift-off length for BDFp. At injection pressure of 100 MPa, BDFc gives shorter lift-off length, but BDFc and diesel give similar equivalence ratio. This is attributed to low  $(A/F)_{st}$  value of BDFc. At injection pressure of 200 MPa, BDFc gives lower equivalence ratio than diesel due to long lift-off length and low  $(A/F)_{st}$ .

At both injection pressures, BDFp shows much lower oxygen ratio at the position of lift-off length because of much higher equivalence ratio. At low injection pressure (100 MPa), BDFc and diesel show a comparable oxygen ratio. At high injection pressure (200 MPa), BDFc gives higher oxygen ratio than diesel due to low equivalence ratio and  $(A/F)_{st}$  for BDFc.

The analysis suggests that different air entrainment characteristics upstream of lift-off length for BDFp are mainly attributed to short lift-off length and small spray angle. The short lift-off length is related to high Cetane number, and the small spray angle is related to high viscosity. Difference air entrainment characteristics upstream of lift-off length plays a significant influence on the combustion in the fuel-rich partially premixed reaction zone and soot formation processes downstream of this

rich central reaction zone.

### **3.5 Relationship among vaporization, combustion and soot formation.**

Pickett and Siebers found that the distance from lift-off length to the region of soot formation would depend strongly on fuel type, and soot tendency of fuel was consistent with this soot formation distance [13]. Long distance indicates a low soot formation tendency. The region of soot formation is detected from soot luminosity with the same experimental conditions [28].

Fig. 11 shows the soot formation distance of three fuels. The longest distance is presented for BDFc. BDFp gives an appreciably longer soot formation distance than diesel at injection pressure of 100 MPa. At injection pressure of 200 MPa, BDFc still gives the longest soot formation distance and BDFp give a much longer distance than diesel.

The comparison of liquid length and lift-off length suggests that there are two distinct relationships between fuel liquid phase and combustion zones. For three fuels at 100 MPa and BDFp at 200 MPa, liquid phase tip is surrounded by diffusion combustion sheath. The cold core, which is blocked to entrain ambient air by the flame sheath, may lead to high soot level. For diesel and BDFc of 200 MPa, fuel vaporization is completely finished prior to combustion. This is beneficial to soot reduction. For diesel and BDFp at injection pressure of 200 MPa, BDFp gives longer soot formation distance than diesel although direct interaction between fuel liquid phase and combustion regions exists for BDFp spray flame. Moreover, air entrainment estimation suggests that BDFp has a poor air entrainment upstream of lift-off length compared to BDFc and diesel. This might lead to higher soot level for BDFp if other factors are neglected. However, BDFp and BDFc respectively gives appreciably and much longer soot formation distances than diesel at injection pressures of 100 and 200 MPa. This reveals the significance of oxygen in biodiesel fuel on soot reduction compared to the oxygen from entrained air. This also suggests that the improved spray atomization for 200 MPa

enhances the significance of oxygen in biodiesel fuels.

## **4 Conclusions**

Experiments were conducted to investigate spray, ignition and combustion characteristics of biodiesel fuels under a simulated diesel-engine condition (885K, 4MPa). Two biodiesel fuels originated from palm oil (BDFp) and used cooking oil (BDFc) were used while JIS#2 used as base fuel. The injection pressures of 100 and 200 MPa were adopted. The results are summarized as follow:

(1) Biodiesel fuels give longer liquid lengths than diesel. The difference of liquid length between biodiesel and diesel is increased as injection pressure is increased.

(2) Biodiesel fuels show shorter ignition delay than diesel and BDFp gives the shortest ignition delay.

(3) BDFp shows the shortest lift-off length at both injection pressures, and the difference of lift-off length between BDFc and diesel is small.

(4) Estimation of air entrainment shows that BDFp gives the lowest oxygen ratio at the position of lift-off length. At injection pressure of 100 MPa, BDFc and diesel give a comparable oxygen ratio. While at injection pressure of 200 MPa, BDFc shows higher oxygen ratio than diesel.

## **Acknowledgements**

Technical support for this study was provided by ISUZU Advanced R&D Center. The properties of biodiesel fuels were measured by Nisseki Oil Company. This study was performed in Spray and Combustion Laboratory, University of Hiroshima, Japan.

## **References**

[1] J. E. Dec, A. O. zur Loye, D. L. Siebers, *SAE Paper* 910224, 1991.

[2] J. E. Dec, *SAE Paper* 920115, 1992.

- [3] J. E. Dec, *SAE Paper* 970873, 1997.
- [4] B. S. Higgins, D. L. Siebers, A. Aradi, *SAE Paper* 2000-01-0940, 2000.
- [5] J. E. Dec, C. Espey, *SAE paper* 982685, 1998.
- [6] D. L. Siebers, *SAE Paper* 980809, 1998.
- [7] J. D. Naber, D. L. Siebers, *SAE Paper* 960034, 1996.
- [8] B. S. Higgins, C. J. Mueller, D. L. Siebers, *SAE Paper* 1999-01-0519, 1999.
- [9] D. L. Siebers, *SAE Paper* 1999-01-0528, 1999.
- [10] D. L. Siebers, B. S. Higgins, *SAE Paper* 2001-01-0530, 2001.
- [11] D. L. Siebers, B. S. Higgins, L. M. Pickett, *SAE Paper* 2002-01-0890, 2002.
- [12] L. M. Pickett, and D. L. Siebers, *SAE paper* 2003-01-3080, 2003.
- [13] L. M. Pickett, and D. L. Siebers, *Int. J. Engine Res.* 7 (2006) 103-130.
- [14] L. M. Pickett, D. L. Siebers, and C. A. Idicheria, *SAE paper* 2005-01-3843, 2005.
- [15] R. L. McCormick, M. S. Graboski, T. L. Alleman, and A. M. Herring, *J. Environ. Sci. Technol.* 35 (2001) 1742 – 1147.
- [16] A. Monyem, , and J. H. V. Gerpen, *Biomass Bioenergy* 20 (2001) 317–325.
- [17] N. Nadi, S. Akhter, and Z. Shahadat, *Bioresour. Technol.* 97 (2006) 372–378.
- [18] D. Laforgia, and V. Ardito, *Bioresour. Technol.* 51 (1995) 53–59.
- [19] A. Senatore, M. Cardone, V. Rocco, and M. V. Prati, *SAE Paper* 2000-01-0691, 2000.
- [20] R. L. McCormick, J. D. Ross, and M. S. Graboski, *Environ. Sci. Technol.* 31 (1997), 1144-1150.
- [21] R. L. McCormick, J. R. Alvarez, M. S. Graboski, K. S. Tyson, and K. Vertin, *SAE Paper* 2002-01-1658, 2002.
- [22] W. Zhang, K. Nishida, J. Gao, and D. Miura, *Proc. Inst Mech Eng, J. Automob Eng* 22 (2008) 1731-1741.

- [23] C. S. Lee, S. W. Park, and S. I. Kwon, *Energy Fuels* 19 (2005) 2201-2208.
- [24] X. L. He, Y. H. Zhan, S. S. Li, *Internal Combustion Engine Fuels*, Sinopec Co. Press, Beijing, 1999, p. 572 (in Chinese).
- [25] R. E. Canaan, J. E. Dec, R. M. Green, and D. T. Daly, *SAE Paper* 980510, 1998.
- [26] P. F. Flynn, R. P. Durett, G. L. Hunter, A. O. zur Loye, O. C. Akinyemi, J. E. Dec, and C. K. Westbrook, *SAE Paper* 1999-01-0509, 1999.
- [27] C. Crua, D. A. Kennaird, S. S. Sazhin, and M. R. Heikal, *Int. J. Engine Res.* 5 (2004) 365-374.
- [28] X. G. Wang, O. A. Kutti, W. Zhang, K. Nishida, Z. H. Huang, *Combust. Sci. Technol. in press*.
- [29] C. J. Mueller, W. J. Pitz, L. M. Pickett, G. C. Martin, D. L. Siebers, and C. K. Westbrook, *SAE paper* 2003-01-1791, 2003.

Table 1 Fuel properties and composition.

Fuel type	Diesel	BDFp	BDFc
Density(15°C)/ $kg/m^3$	830	874.4	885.1
Viscosity(30°C)/ $mm^2/s$	3.36	5.53	4.45
Surface tension/mN/m	25.5	26.2	25.7
Cetane number	55	64.6	49.9
Heating value/ $MJ/kg$	43.1	40.03	39.03
Carbon content/ $wt\%$	86.1	76.5	77.1
Hydrogen content/ $wt\%$	13.8	12.3	12.0
Oxygen content/ $wt\%$	<1	11.1	10.6
$(A/F)_{st}$	14.69	12.59	12.58

## **List of Figure Captions**

Fig. 1 Experimental apparatus.

Fig. 2 Samples of spray development process for BDFp.

Fig. 3 Liquid length of each condition.

Fig. 4 Samples of ignition process for BDFp.

Fig. 5 Ignition delay of each condition.

Fig. 6 Variation of OH luminosity area versus elapsed time.

Fig. 7 OH intensity profiles along the injector axial line (1.5 ms ASOI).

Fig. 8 Samples of lifted jet flame and measurement of lift-off length for BDFp at injection pressure of 100 MPa.

Fig. 9 Lift-off and liquid lengths of each condition.

Fig. 10 Equivalence ratio and oxygen ratio of each condition.

Fig. 11 Soot formation distance of each condition.



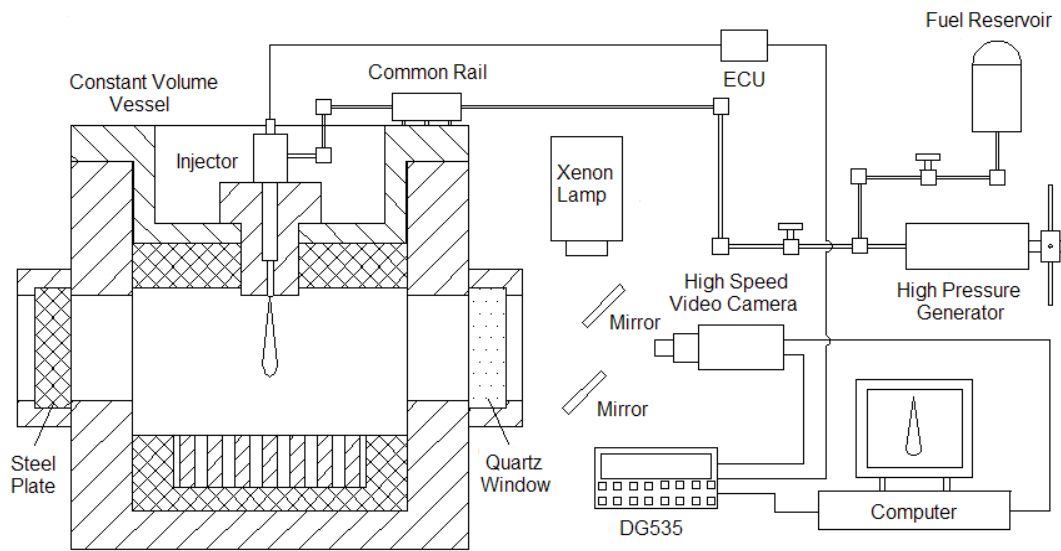


Fig. 1 Experimental apparatus.

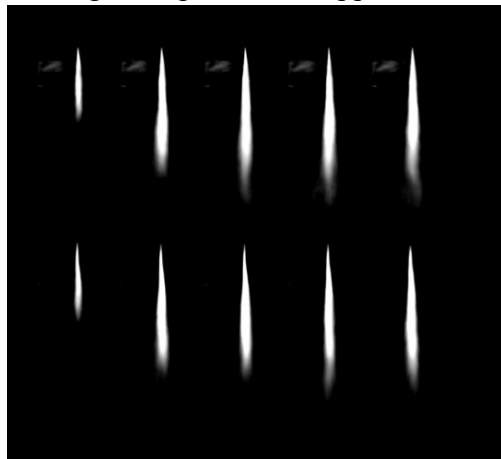


Fig. 2 Samples of spray development process for BDFp.

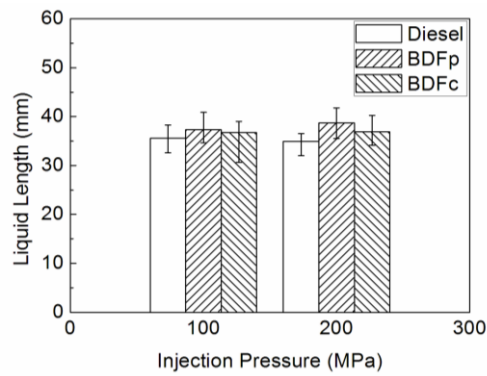


Fig. 3 Liquid length of each condition.

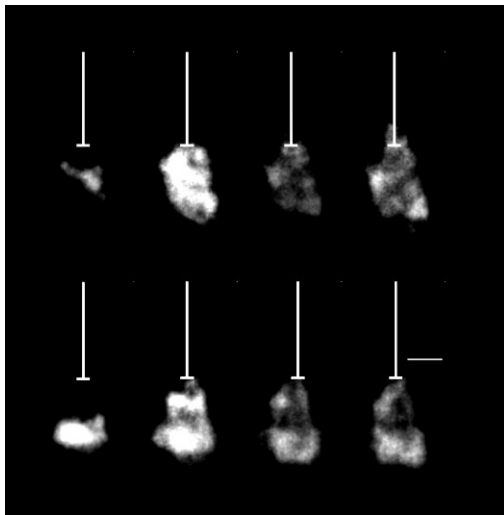


Fig. 4 Samples of ignition process for BDFp.

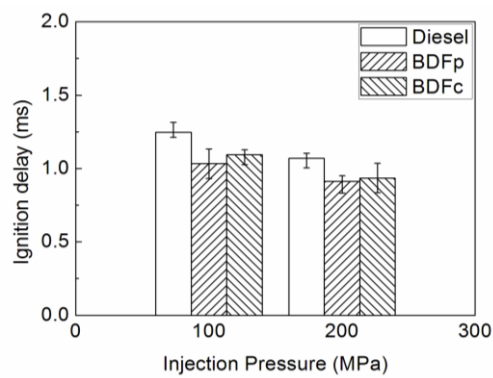


Fig. 5 Ignition delay of each condition.

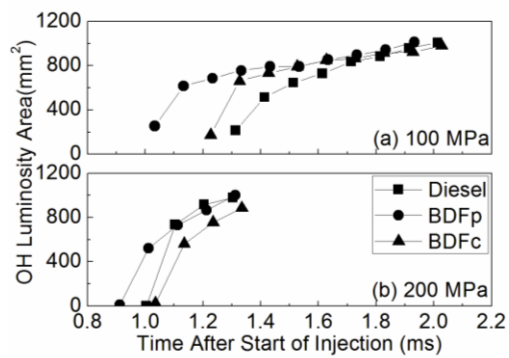


Fig. 6 Variation of OH luminosity area versus elapsed time.

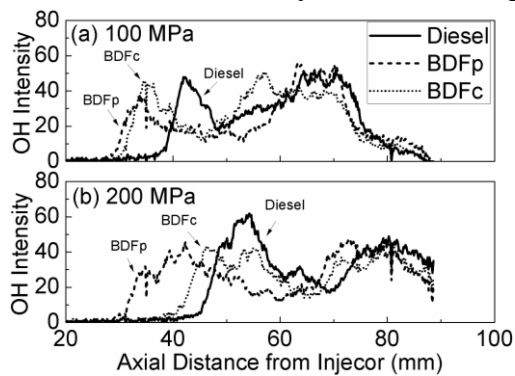


Fig. 7 OH intensity profiles along the injector axial line (1.5 ms ASOI).

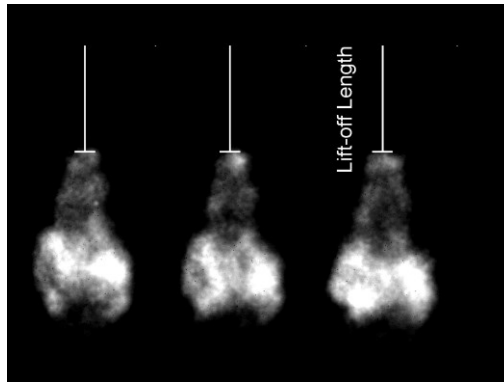


Fig. 8 Samples of lifted jet flame and measurement of lift-off length for BDFp at injection pressure of 100 MPa.

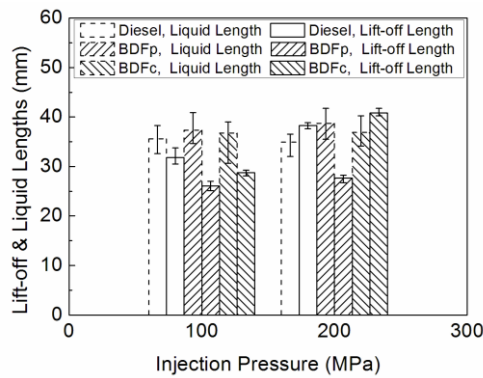


Fig. 9 Lift-off and liquid lengths of each condition.

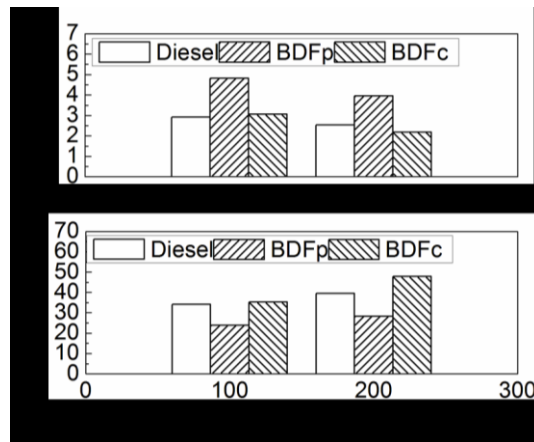


Fig. 10 Equivalence ratio and oxygen ratio of each condition.

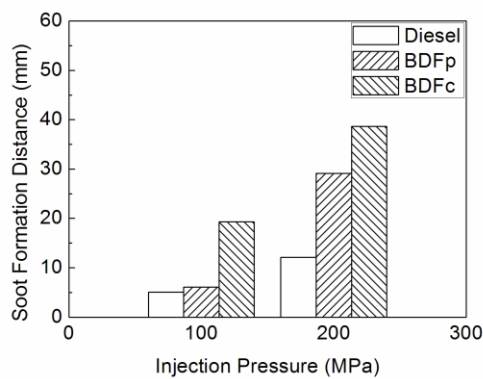


Fig. 11 Soot formation distance of each condition.